AIAA SciTech Forum
8-12 January 2024, Orlando, FL
AIAA SCITECH 2024 Forum

10.2514/6.2024-2046

Determining Mechanical Properties of Thermally Sprayed Coatings Through Synchrotron X-Ray Diffraction Measurements

Perla Latorre-Suarez* and Zachary Stein†
Embry-Riddle Aeronautical University, Daytona, Florida, USA

Quentin Fouliard‡
University of Central Florida, Orlando, Florida, USA

Janine Wischek§ and Marion Bartsch¶
Institute of Materials Research, German Aerospace Center, Cologne, Germany.

Peter Kenesei, Jun-Sang Park, Jonathan Almer‖ and Jonathan Almer**
Advanced Photon Source, Argonne National Laboratory, Lemont, USA.

Seetha Raghavan††
Embry-Riddle Aeronautical University, Daytona, Florida, USA

Thermally sprayed ceramic coatings are commonly used in the aerospace and power generation industry as a protective material for a variety of substrates. The mechanical properties of the coating material are crucial for maintaining the protective functionality of the coating. The material response to external loads is highly influenced by residual stresses developed during the deposition process of the thermally sprayed coating, affecting apparent mechanical properties such as Young's modulus, hardness, adherence, and wear resistance. Synchrotron X-ray diffraction offers a means to capture in-situ strain data during the indentation process on the surface of the coating. In this study, the Rockwell hardness test has been paired with high-energy X-ray diffraction to study the mechanical behavior of an alumina coating applied on an aluminum substrate by air plasma spraying. The indented coating was evaluated via high-energy X-ray diffraction at 0, 160, 315, and 580 N of indentation load. The strain analysis was performed in two directions, the in-plane (e_{11}) and out-of-plane (e_{22}). A significant strain change was observed when increasing the indentation load from 315 N to 580 N. The results indicated strain relief, which can be associated with damage evolution, such as crack formation.

*Graduate Student, Aerospace Engineering, Embry-Riddle Aeronautical University and AIAA Student Member
†Graduate Student, Aerospace Engineering, Embry-Riddle Aeronautical University and AIAA Student Member
‡Postdoctoral Researcher, Mechanical and Aerospace Engineering, University of Central Florida, AIAA Member
§Group Leader of Mechanical Testing of Materials Laboratory, Institute of Materials Research, German Aerospace Center, Cologne, Germany.
¶Department Head of Experimental and Numerical Methods, Institute of Materials Research, German Aerospace Center, Cologne, Germany.
‖Beamline Scientist, Advanced Photon Source, Argonne National Laboratory, Lemont, USA .
**Group Leader, Materials Physics and Engineering Group, Advanced Photon Source, Argonne National Laboratory, Lemont, USA .
††Associate Dean, Aerospace Engineering, Embry-Riddle Aeronautical University, AIAA Associate Fellow, seetha.raghavan@erau.edu.

I. Introduction

Thermally sprayed materials are frequently used in the aerospace and power generation industry as protective coatings for components in the hot sections of gas turbines. One of the most common methods of thermal spraying is Air Plasma Spray (APS), which allows the processing of metallic and ceramic materials and depositing layers of several millimeter thickness. However, thermally sprayed coatings, such as APS coatings, result in an anisotropic lamellar structure, as illustrated in Figure 1. This structure can initiate delamination, which might be accompanied by intra-lamella microscopic cracks [1]. Mechanical properties such as elastic modulus, fracture toughness, and interfacial fracture toughness at the interface must be determined to evaluate the endurance of the APS coatings and the adherence of the coatings to the substrate. The evaluation process of these mechanical properties is challenging due to the anisotropy and the porosity of APS-processed materials [2]. Furthermore, residual stresses have to be considered, which evolve in the layered material system as a consequence of thermal misfit between the substrate and coating materials.

Indentation and scratch tests have been utilized to achieve information about the local material properties [3]. The mechanical properties of ceramic materials have been investigated through indentation experiments, where indenters with a sharp-edged tip, such as Vickers, Knoop, and Berkovic, are generally used to determine the hardness, bulk modulus, and cracking resistance [4]. On the other hand, spherical indenters, such as Rockwell and Brinell, are mainly used to determine the tensile properties and bulk modulus [5]. It is a challenge to establish the mechanical properties when considering the complex structure of the thermally sprayed coatings. Researchers have investigated the micromechanical response of the ceramic top coat, including the crushing and formation of cracks, through Rockwell hardness experiments and microscopic images to analyze the formation and size of debonding cracks [6]. Indentation hardness measurements are categorized by loading scales, macro-, micro-, and nanoindentation [5]. The macro- and micro-indentation tests focus on determining the materials' resistance to the penetration of a non-deformable indenter and correlate hardness with the depth in which the indenter will sink into the material. The elastic and plastic deformation of the material is observed during the nanoindentation test, where the indenter is pushed into the surface of the samples at lower loads [5].

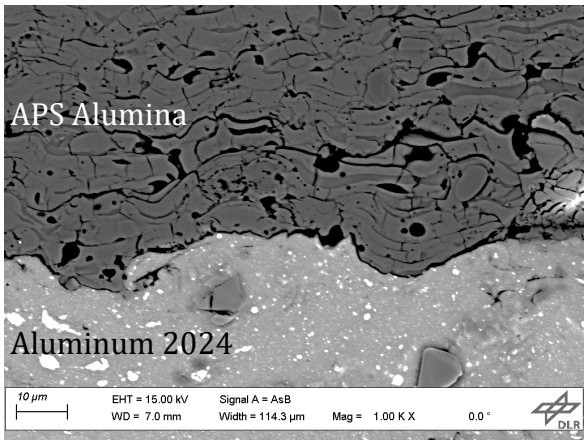

Fig. 1 Scanning electron image of the cross-section of APS alumina displaying the anisotropic lamellar structure of the coating.

For the interpretation of the results of the indentation tests, subsurface information on the compaction of the porous APS material and the formation of cracks is required, but not commonly determined. Evaluation methods, such as microscopic investigations of the damaged features at the indentation location, are time-consuming and do not provide information on the stress or strain state of the material. Further, the sample preparation, namely cutting, grinding, and polishing, changes the stress state of the indented material. In contrast, high energy X-ray diffraction (XRD) is a non-destructive method to acquire information on the elastic strain state and the phase composition of a crystalline material. It has been demonstrated that by employing X-ray diffraction, the strain state is evaluated by determining shifts in the diffraction peaks due to external or residual stresses, and at larger diffraction angles, the sensitivity of the method is higher providing higher precision of strain evaluation [7, 8]. In previous studies, XRD has been used to achieve information on the strain state of aluminum in the vicinity of scratches [9]. Changes in phase composition occur in some materials during indentation testing and have been detected by XRD for partially stabilized yttria-zirconia coating [3]. Using high energy X-rays, as generated in synchrotron facilities, allows even for in-situ measurements of strain changes or phase transitions as a response to thermo-mechanical loading [10–12].

In this work, APS alumina coatings on aluminum substrates with an intermediate bond coat layer composed of nickel, chromium, aluminum, and yttrium (NiCrAlY), in as-coated conditions, were investigated employing high-energy X-rays before and during Rockwell indentation for in-situ monitoring of strain throughout the indentation procedure. Previous work performed in our research laboratory has demonstrated that the roughness of the APS alumina coating increases with the presence of a bond coat and thickness increment [13]. Considering the roughness of the APS alumina coating, a macro-hardness test using a Rockwell indenter was performed in this study, accounting for the rough-surface indentation effect [14].

II. Experimental Procedure

A. Coating Manufacturing

An aluminum 2024 substrate was grit blasted to provide the surface roughness required to improve the mechanical interlocking and to provide a strong adherence during the APS deposition process of the topcoat with the bond coat. APS was then used to deposit a 150 μm layer bond coat with a composition of 67 wt% nickel, 22 wt% chromium, 10 wt% aluminum, and 1 wt% yttrium (NiCrALY) (Praxair, NI164-211, -106/+45 μm) and a 100 μm layer of aluminum oxide (Praxair, ALO-101, median particle size d_{50} = 45 μm), as shown in Figure 2. The bond coat has been applied to the coating system to promote adherence of the ceramic coating to the substrate [15]. Spray parameters, such as spraying distance, substrate temperature, coating thickness, and substrate roughness, typically affect the hardness, porosity, and roughness of the resulting aluminum oxide coating, affecting the material's microstructure. Considering the effect of the spraying parameters on the microstructure of the coating, a distance of 76.2 mm between the spray gun and the sampling point was employed. Plasma was generated through a voltage of 550 V and a current of 39 A, with argon as the primary gas (2.94 m^3/hr) and helium as the secondary gas (1.42 m^3/hr).

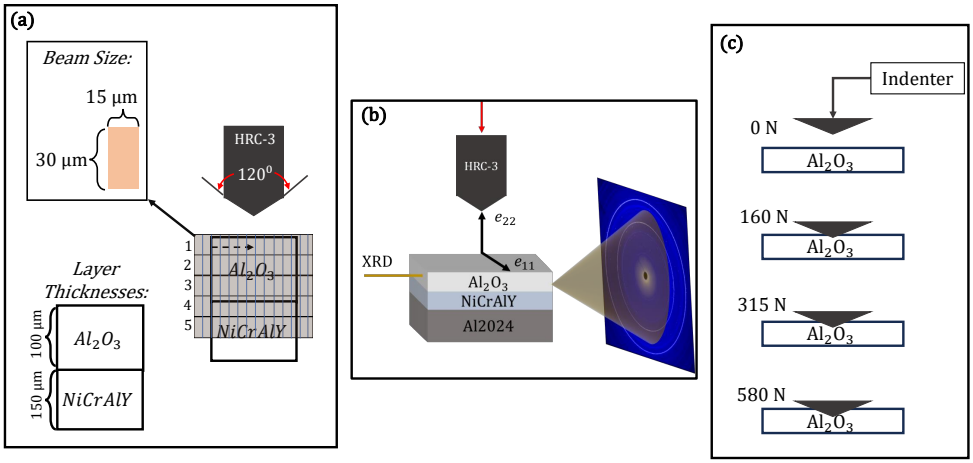

Fig. 2 (a) Schematic of the layer thickness of the top and bondcoat, the beam parameters and location of scans, numbered as lines 1 to 5, taken with the high-energy XRD beam, (b) the direction in which the XRD data was collected with respect to the in-plane, e_{11}, and out-of-plane, e_{22}, strain directions, and (c) loads of the indent performed on the surface of the APS alumina coating while collecting in-situ synchrotron data.

B. Indentation Process and Synchrotron Data Collection

High-energy XRD measurements were performed at beamline 1-ID of the Advanced Photon Source at Argonne National Laboratory. The high-energy XRD information was used to determine material characteristics, such as crystal phase volume fraction, grain size, texture and to quantify of strain. The incident beam cross-section had a width of 15 μm and a height of 30 μm, shown in Figure 2(a), and the beam energy was 90.515 keV. Alignment and calibration of the incident beam were performed using ceria (CeO_2) powder, allowing for accurate measurements of the distance between

the sample and the detector. Figure 2(a) displays the schematic in which the high-energy XRD scans were collected during each load. Scans parallel to the surface with 524 frames for each scan were captured at the five different distances from the coating surface, as shown in Figure 2 (a). The 524 individual frames were collected across the coating, from the left side to the right side, as indicated in the sketch in Figure 2(a). The specimen was indented using a Rockwell indenter (HRC-3) having a conical diamond tip with an angle of 120° displayed in Figure 2(a). The strain directions are displayed in Figure 2(b), where e_{11} is the in-plane strain and e_{22} is the out-of-plane strain. The data sets were acquired after each indentation load at 0, 160, 315, and 580 N without removing the indenter, as shown in Figure 2(c). The beam had a displacement rate of 22 μm/s and an exposure time of 0.3 seconds per frame. Figure 3 displays the setup for the indentation experiment. The specimen was indented using a compact load frame developed in the Advanced Photon Source, Argonne National Laboratory. The specimen was indented to a maximum load of 580 N. High-energy XRD data were collected at each of the previously mentioned loads, enabling the study of changes in the strain state at the indent as a function of indentation load.

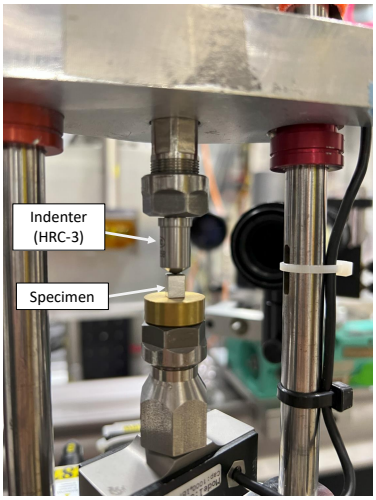

Fig. 3 Compact load frame developed in the Advanced Photon Source, Argonne National Laboratory and Rockwell indenter. The sample was placed on a flat surface while loaded up to 580 N

III. Results and Discussion

XRD data of the APS alumina was acquired before indentation. An XRD lineout of this data is displayed in Figure 4 and shows that the main phases present in the APS alumina coating consisted of alpha (α) and gamma (γ) phase alumina. Previous studies have shown that the APS alumina coatings are composed of stable α-phase and cubic metastable γ-phase [16]. Considering the spraying parameters, the composition of the APS alumina coating may vary. It has been demonstrated that the increase of power input during the spraying process will increase the amount of metastable γ-phase alumina [16]. The strain analysis performed in this study, used the shift in d-spacing of the α-phase in the [116] plane.

The strain, e_{11}, is in the plane of the coating layer, and e_{22} is out of the plane in the direction the indent load was applied. This allowed to determine the strain changes while the load was applied to the coating. In this analysis, the summation of the 524 frames collected at each of the five scans through the depth of the top coat was used to determine the diffraction strain value at each load. A reference orientation value, η^*, of 53.48° was determined through [17]. This η^* value represents an azimuth angle around the Debye-Scherrer at which the radius of the ring is unaffected by strain changes. This radius corresponds to the d-spacing of the unstrained material. Deviation of this radius correlates with XRD strain. Figure 5 shows the strain values calculated at the second point of the XRD scan for each load. The second point of the XRD scan is used in this study as an example to demonstrate the strain changes as the load is applied and consider the minimum indent depth at each load. As shown in the graphs, there is a minor change when increasing the indenter load from 0 N to 160 N. When further increasing the indenter load up to 315 N, strain values increased, indicating an increase of elastic energy stored in the material. Further load increases up to 580 N result in a decrease of the strain values, which can be attributed to the dissipation of energy by damage processes such as compaction of pores

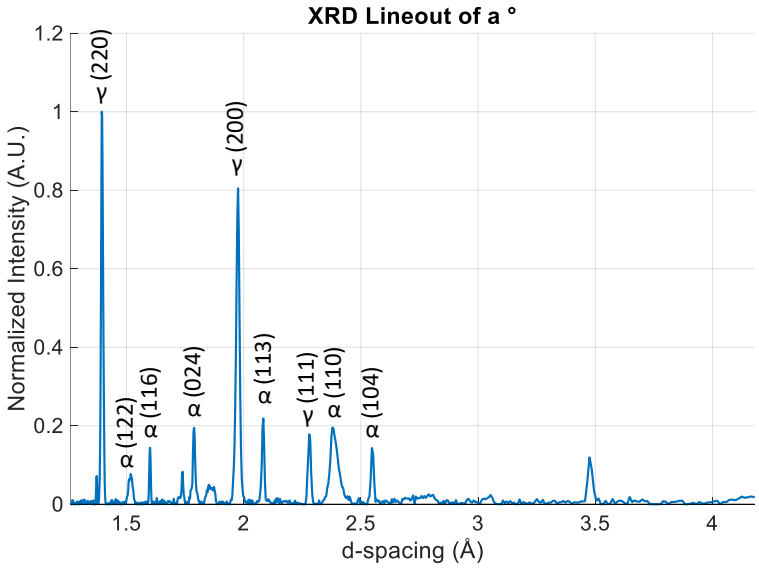

Fig. 4 Exemplary lineout of normalized XRD intensity as a function of d-spacing showing the presence of, gamma (γ) and alpha (α) alumina.

and initiation of cracks.

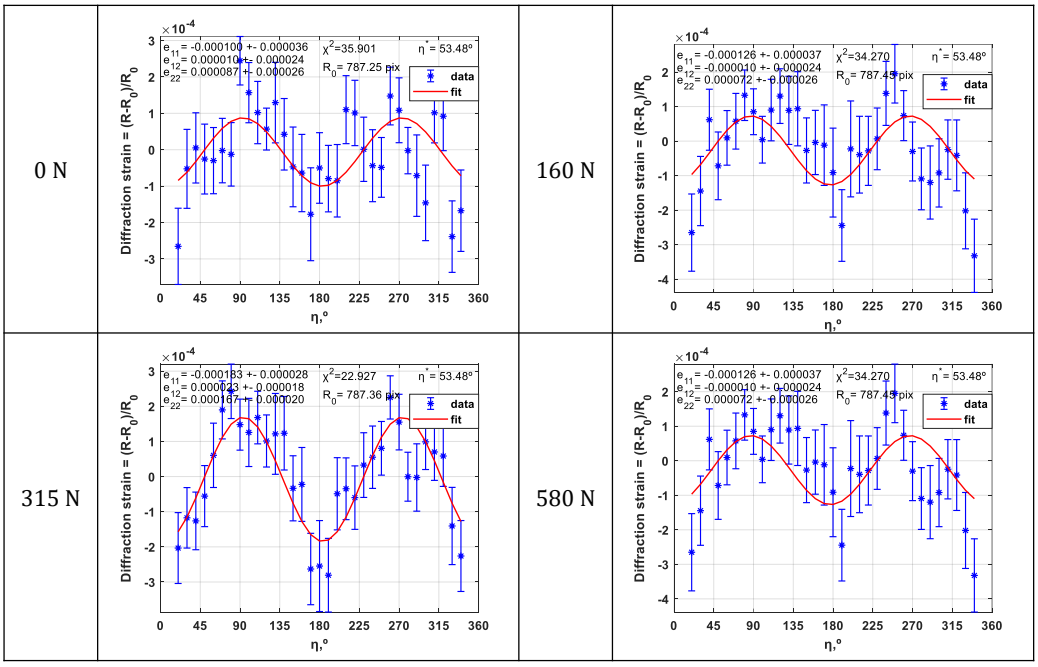

Fig. 5 Summation of the frames collected at the second point scan through high-energy XRD to determine the strain values at each load considering the minimum indented depth through the surface of the coating.

Figure 6 displays graphs showing the average XRD strain values in the e_{11} and e_{22} direction, which were determined

from the summation of the frames and average of the five scans performed during each load applied. The standard deviation of the determined XRD strains is indicated in the graphs and displayed as error bars. At 0 N indentation load, XRD strain is observed, which is attributed to the residual strain evolving due to the processing conditions when the coating is deposited and cooled to ambient temperature. As the indentation load was increased to 315 N, the compressive in-plane strain e_{11} increased, and a significant decrease occurred after the next load step to 580 N. The corresponding out-of-plane strain e_{22} stayed nearly constant in the first load step until 160 N, increased when further loading up to 315 N was applied, and decreased again when the maximum load of 580 N was applied. The strain increase in the first load steps can be attributed to an increment in elastic strain energy due to elastic deformation when starting the indentation process. The strain relief during further loading can be explained by energy-dissipating damage processes like pore compaction in the porous coating and crack formation.

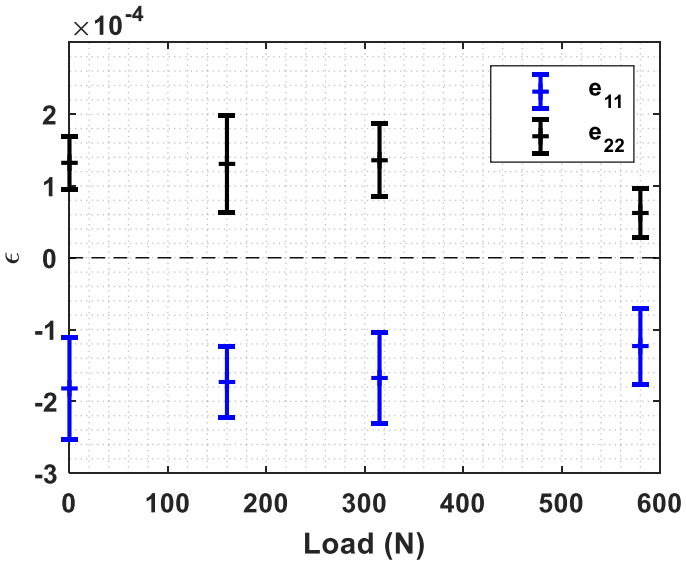

Fig. 6 Average of XRD strain values e_{11} and e_{22} determined from frames of all scans in dependence of the indentation load. The standard deviation is indicated

IV. Conclusion

Using high-energy X-ray diffraction, the damage evolution of the APS alumina coating has been observed in-situ during indentation through strain measurements. The APS alumina coating behavior was tested to study the strain changes at the coating. The high-energy XRD results demonstrated the presence of γ- and α-phase alumina due to the spraying parameters used during the APS deposition. The strain changes across the coating were monitored through the high-energy XRD measurements while in-situ indentation at 160, 315, and 580 N loads. The strain values were calculated parallel to the surface of the APS alumina coating, e_{11}, and in indentation direction, e_{22}. The summation of the frames and the average of the scans, neglecting the indentation depth, demonstrated that the strain values in the e_{11} direction became less compressive, and at the e_{22} less tension, indicating stress relaxation. Further analysis will be performed to study the indentation depth and correlate the results with the high-energy XRD values. This work enables the study of mechanical properties in thermally sprayed materials using a small material volume, which can be analyzed through non-destructive methods like high-energy XRD.

Acknowledgments

This material was based upon work supported by the National Science Foundation grants OISE 1952523 and by the German Aerospace Center (DLR). Use of the Advanced Photon Source, an Office of Science User Facility operated for the US Department of Energy (DOE) Office of Science by Argonne National Laboratory, was supported by the US DOE under contract No. DE-AC02- 06CH11357. Mr. Frank Accornero and Dr. Mary McCay (Applied Research Laboratory, Florida Institute of Technology) are acknowledged for their support with the air plasma spray coating deposition.

References

[1] Odhiambo, J. G., Li, W., Zhao, Y., and Li, C., "Porosity and its significance in plasma-sprayed coatings," *Coatings*, Vol. 9, No. 7, 2019, p. 460.

[2] Yin, Z., Tao, S., Zhou, X., and Ding, C., "Evaluating microhardness of plasma sprayed Al2O3 coatings using Vickers indentation technique," *Journal of Physics D: Applied Physics*, Vol. 40, No. 22, 2007, p. 7090.

[3] Munoz-Tabares, J., Jiménez-Piqué, E., Reyes-Gasga, J., and Anglada, M., "Microstructural changes in 3Y-TZP induced by scratching and indentation," *Journal of the European Ceramic Society*, Vol. 32, No. 15, 2012, pp. 3919–3927.

[4] Chicot, D., Tricoteaux, A., et al., "Mechanical properties of ceramics by indentation: Principle and applications," *Ceramic Materials*, 2010, pp. 115–153.

[5] Broitman, E., "Indentation hardness measurements at macro-, micro-, and nanoscale: a critical overview," *Tribology Letters*, Vol. 65, No. 1, 2017, p. 23.

[6] Yan, J., Leist, T., Bartsch, M., and Karlsson, A. M., "On cracks and delaminations of thermal barrier coatings due to indentation testing: Experimental investigations," *Acta materialia*, Vol. 56, No. 15, 2008, pp. 4080–4090.

[7] Irizalp, S. G., and Saklakoglu, N., "1.14 Laser Peening of Metallic Materials," *Comprehensive Materials Finishing*, Elsevier Oxford, 2017, pp. 408–440.

[8] Prevéy, P. S., et al., "X-ray diffraction residual stress techniques," *ASM International, ASM Handbook.*, Vol. 10, 1986, pp. 380–392.

[9] Khan, M., Fitzpatrick, M. E., Edwards, L., and Hainsworth, S., "Determination of the Residual Stress Field around Scratches Using Synchrotron X-Rays and Nanoindentation," *Materials Science Forum*, Vol. 652, Trans Tech Publ, 2010, pp. 25–30.

[10] Knipe, K., Manero, A., Siddiqui, S. F., Meid, C., Wischek, J., Okasinski, J., Almer, J., Karlsson, A. M., Bartsch, M., and Raghavan, S., "Strain response of thermal barrier coatings captured under extreme engine environments through synchrotron X-ray diffraction," *Nature communications*, Vol. 5, No. 1, 2014, p. 4559.

[11] Manero, A., Sofronsky, S., Knipe, K., Meid, C., Wischek, J., Okasinski, J., Almer, J., Karlsson, A. M., Raghavan, S., and Bartsch, M., "Monitoring local strain in a thermal barrier coating system under thermal mechanical gas turbine operating conditions," *JOM*, Vol. 67, 2015, pp. 1528–1539.

[12] Stein, Z., Naraparaju, R., Schulz, U., Kenesei, P., Park, J.-S., Almer, J., and Raghavan, S., "Synchrotron X-Ray Diffraction Study of Phase Transformation in CMAS Ingressed EB-PVD Thermal Barrier Coatings," *AIAA Scitech 2020 Forum*, 2020, p. 0400.

[13] Latorre-Suarez, P., Fouliard, Q., Wohl, C., Wiesner, V., and Raghavan, S., "Measuring the Wear and Abrasive Resistance of Air Plasma Sprayed Aluminum Oxide for Lunar Exploration," *74th International Astronautical Congress (IAC)*, 2023.

[14] Kim, J.-Y., Kang, S.-K., Lee, J.-J., Jang, J.-i., Lee, Y.-H., and Kwon, D., "Influence of surface-roughness on indentation size effect," *Acta materialia*, Vol. 55, No. 10, 2007, pp. 3555–3562.

[15] Viswanathan, V., Lance, M. J., Haynes, J. A., Pint, B. A., and Sampath, S., "Role of bond coat processing methods on the durability of plasma sprayed thermal barrier systems," *Surface and Coatings Technology*, Vol. 375, 2019, pp. 782–792.

[16] Misra, V. C., Chakravarthy, Y., Khare, N., Singh, K., and Ghorui, S., "Strongly adherent Al2O3 coating on SS 316L: Optimization of plasma spray parameters and investigation of unique wear resistance behaviour under air and nitrogen environment," *Ceramics International*, Vol. 46, No. 7, 2020, pp. 8658–8668.

[17] Manns, T., and Scholtes, B., "DECcalc-A program for the calculation of diffraction elastic constants from single crystal coefficients," *Materials Science Forum*, Vol. 681, Trans Tech Publ, 2011, pp. 417–419.